RSC Advances

ROYAL SOCIETY OF CHEMISTRY

www.rsc.org/advances

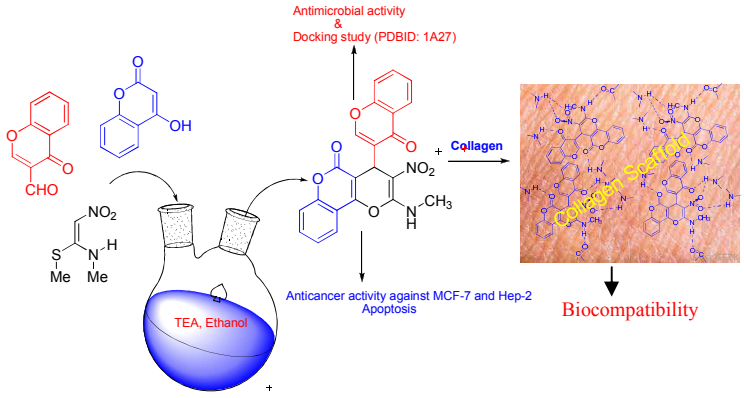

A one pot domino protocol has been developed for the efficient synthesis of novel chromen and pyrano chromen-5-one derivatives. The synthesis was achieved by reaction of 4-Hydroxycoumarin, Chromene-3-carbaldehyde and NMSM in the presence of triethylamine in ethanol. The combination of ethanol triethylamine has obtained excellent results in simple experimental method. The product (CCN) and collagen based scaffold showed excellent biological properties to act as biomaterial in tissue engineering and biomedical application.

RSC Advances

ARTICLE

Synthesis, characterization and biological evaluation of chromen and pyrano chromen-5-one derivatives impregnated into a novel collagen based scaffold for tissue engineering application†

Received 00th January 20xx,
Accepted 00th January 20xx

DOI: 10.1039/x0xx00000x

www.rsc.org/

Subramani Kandhasamy[a], Giriprasath Ramanathan[b], Jayabal Kamalraja[a], Ravichandran Balaji[c], Narayanasamy Mathivanan[c], Uma Tiruchirapalli Sivagnanam[b]*and Paramasivan Thirumalai Perumal[a]*

Abstract

In this article, we describe the synthesis and biological evaluation of a novel 2-(methylamino)-3-nitro-4-(4-oxo-4H-chromen-3-yl) pyrano[3,2-c]chromen-5(4H)-one (CCN). It is also determined that CCN impregnated into the collagen scaffold has the potential to mimic the function of the extracellular matrix as a biomaterial in the field of tissue engineering. The series of pyrano[3,2-c]chromen-5(4H)-one derivatives (4a-4j), were analyzed by ^{1}H NMR, ^{13}C NMR, Mass spectral and FTIR analysis. The compound 4c confirmed by single crystal XRD studies. All the compounds were screened for antimicrobial activity against the gram positive, gram negative bacteria and yeast. Among all the compounds, the compound (4a=CCN) showed activity against Gram positive and Gram negative bacteria, when compared to the synthesized compounds. Further the compound CCN was evaluated for cytotoxicity against MCF-7, Hep-2 and Vero cancer cell lines with IC50 values of 5.4 µg/ml, 5.3 µg/ml and 68.4 µg/ml respectively. In addition, the result of flow cytometry and docking ((PDBID: 1A27 with the ligand) study were supported to the activity of the synthesized compound (4a). The FTIR and NMR analysis of the CCN impregnated collagen scaffold were done to reveal the existence of CCN molecule in the scaffold. The inherent property of the collagen scaffold was not significantly affected by structure of CCN molecule. The thermal and mechanical properties of the collagen scaffold impregnated with CCN molecule gives stability as well as supports the swelling. However, the COL-CCN scaffold showed an enhanced cell attachment and proliferation of NIH 3T3 fibroblast cells. Based on the results, the novel CCN molecule impregnated with collagen scaffold has the potential application as a biomaterial in tissue engineering.

Introduction

Collagen scaffold as biomaterial gives the structural support for the development of scaffold with unique properties in the tissue engineering field. Collagen is one of the main structural and functional proteins, which has shown innovations in the field of tissue engineering superior biomedical applications[1,2]. Tissue engineering is an emerging field offering novel perspective in the treatment of damaged or diseased organs[3,4]. Tissue engineering mostly requires that material to be biocompatible[5], nontoxic[6], low antigenicity[7] and noninflammatory[8,9], which is more important to design and develop a degradable material based on collagen[10,11]. The application of the collagen scaffold material for tissue engineering field[12] with cell attachment and proliferation makes the scaffold to function as extra cellular matrix[13]. The bioactive molecule impregnated with collagen have been used to enhance the stability of the scaffold[14,15]. Collagen scaffolds mimic the function of extracellular matrix (ECM) to support collagen matrix synthesis, cell proliferation[16] and also examines the signs of fibroblast activation[17,18]. Recently bioactive molecules have functionalized with collagen to form thin film or scaffold as a biomaterial[19,20]. Mostly individual collagen does not possess antimicrobial property, but the combination of synthetic molecule collagen showed progress towards biocompatibility in biomedical applications. Bioactive molecules[21] concerned with collagen have enhanced in various tissue engineering application[22]. Coumarin forms an important source of cassia cinnamon, (class of benzopyrones) which is found in nature[23,24]. Coumarin and their functionalized derivatives possess a vital role in biological activities as a potent anti-HIV, anticancer[25], anti-inflammatory[26], antimicrobial[27], antidiabetic, and clinically used antifungal drugs[28,29]. Number of researches have also enlisted that a coumarin based drug has highly selective and non toxic

[a] Organic Chemistry Division, CSIR-Central Leather Research Institute, Adyar, Chennai-600020, Tamilnadu, India. E-mail: ptperumal@gmail.com, Tel: + 91 44 24437223; Fax: +91 44 24911539
[b] Bioproducts Lab, CSIR-Central Leather Research Institute, Chennai-600020, Tamilnadu, India. E-mail: suma67@gmail.com; Tel: + 91 44 24420709; Fax: +91 44 24911589
[c] Biocontrol and Microbial Metabolites Lab, Centre for Advanced Studies in Botany, University of Madras, Maraimalai Campus, Guindy, Chennai – 600 025, Tamilnadu, India.

† Footnotes relating to the title and/or authors should appear here.
Electronic Supplementary Information (ESI) available: ^{1}Hand^{13}C NMR and ESI-HRMS Spectrum of all compounds
CCDC 1055442, crystallographic data in CIF
. See DOI: 10.1039/x0xx000x 00

pharmaceuticals in tissue engineering application[30]. On the other hand, Chromen ring acts as essential chromophore in recent drug discovery. It consists of very important class of flavonoids, alkaloids, and anthrocyanins which are present naturally[31]. Chromen scaffold with collagen has induced inhibitory of activities against human platelet aggregation[32,33] which form the backbone with a combination of peptides, polymers and carboxylate derivatives with various groups[34,35]. However, great efforts have been put to concentrate the development of coumarin and chromen as potential therapeutic in biomedical applications[36,37]. Therefore, in literature survey, the coumarin and chromen moieties impregnated with polymers and peptides have been used valid tissue scaffold in medicinal chemistry which has focused on the development of tissue engineering and biomedical application[38-41].

We herein report a novel and an efficient synthesis of 2-(methylamino)-3-nitro-4-(4-oxo-4H-chromen-3-yl)pyrano[3,2c] chromen-5(4H)-one (CCN) derivatives via domino knoevenagel condensation/ Michael addition/ intramolecular O-cyclization reactions of 4-Hydroxycoumarin and Chromene-3-carbaldehyde with NMSM (Scheme 1). The synthetic molecules possess highly bioactive moiety which are coumarin and Chromen derivatives. The entire 10 compounds were screened for antimicrobial activity against Gram positive bacteria, Gram negative bacteria and yeast. Further the cytotoxicity against MCF-7 and Hep-2 cancer cell lines were evaluated for CCN molecule. The compound as moderate DNA laddering on the DNA of tested cells therefore, it is suggested that the mechanism of action of this compound involves apoptosis.

The potential biological application of the bioactive molecule provoked the knowledge in the tissue engineering field for the application CCN impregnated collagen scaffold. Based on the consideration of above mentioned moiety (CCN) has successfully involved in providing antimicrobial activity and stability to the collagen scaffold. Therefore, the collagen and bioactive molecules have combined together via inter molecular hydrogen bonding[42] to enforce alignment of the designed collagen scaffold.

In this manuscript, we synthesized 2-(methylamino)-3-nitro-4-(4-oxo-4H-chromen-3-yl)pyrano[3,2-c]chromen-5(4H)-one derivatives and collagen banded together for the development of collagen scaffold and evaluated their antimicrobial, cytotoxicity against anticancer activity(apoptosis) and molecular docking study. The thermal and mechanical studies of the collagen scaffold, swelling and degradation rate with enhanced cell attachment and proliferation of NIH 3T3 fibroblast cells. MTT assay and *in vitro* studies of fibroblast cell line for tissue engineering application.

To the best of our knowledge, there is no work designed which studies the influence of synthetic compound, 2-(methylamino)-3-nitro-4-(4-oxo-4H-chromen-3-yl)pyrano[3,2-c]chromen-5(4H)-one (CCN) used for generating collagen based scaffold in tissue engineering application. Herein, we report for the first time the use of synthetic compound for novel collagen merged biomaterial.

Experimental section

The *Arothron stellatus* fish was collected from the deep sea in the Bay of Bengal region in Nagapattinam, Tamil Nadu, India. Tris HCl, Tris buffer, Glycine, Dulbecco's modified Eagle's medium (DMEM), Fetal bovine serum (FBS) and supplementary antibiotics for tissue culture were purchased from Sigma Aldrich, India. The mouse NIH 3T3 fibroblast, MCF-7 and Hep-2 cancer cell lines were obtained from the National Centre for Cell Science (NCCS), Pune, India.

Synthesis of 2-(methylamino)-3-nitro-4-(4-oxo-4H-chromen-3yl)pyrano[3,2-c]chromen-5(4H)-one derivatives

First, we initiated. **1** 4-Hydroxycoumarin (0.81g, 5mmol), **2** Chromene-3-carbaldehyde (0.87g, 5mmol), and **3** NMSM (0.74g, 5mmol) were selected as substrate to the reaction. Initially, the above three component coupling was carried out in EtOH at room temperature in the presence of TEA (Triethylamine 0.1eq), as a catalyst. Upon completion of the reaction, the mixture was filtered, and washed with ethanol to obtain the desired product. The combination of ethanol triethylamine has obtained excellent results in the experiments. The overall yield was 83% obtained.

Extraction of collagen from Arothron stellatus skin

All the preparative procedures were conducted at 4°C in the cold room. The obtained fish skin was washed plenty of time to remove the adherent blood particles and was chopped into small pieces. Then methanol and chloroform mixture (3:1) ratio were added to remove fat. Initially, skin pieces were soaked for 3 days in 0.5 M acetic acid followed by removal of epidermal layer from the skin. The skin pieces were again soaked with fresh volumes of acetic acid for another 3 days. Then the swollen dermal skin pieces were homogenized with 0.5 M acetic acid using the Homogenizer (Ultra Turax T-50, IKA Werke, Germany). Then the homogenized skin was centrifuged at 8000 rpm for 30 min at 4°C. The resultant mixture was salted out by adding NaCl to a final concentration of 0.7 M, followed by precipitation of the collagen by the addition of NaCl (final concentration of 2.3 M) in 0.05 M Tris–HCl (pH 7.5). The precipitated mixture was separated by centrifugation at 8000 rpm for 30 min at 4°C, and then dialyzed against 0.1 M acetic acid and distilled water in subsequent days to obtain *Arothron Stellatus* fish skin collagen.[43, 44] The collagen was washed with distilled water, and then lyophilized (Operon Co., Korea)

Fabrication of collagen scaffold impregnated with the CCN molecule (COL-CCN)

Collagen (COL) scaffold was prepared by pouring 50 ml of 4 wt % collagen solutions into polyethylene tray (measuring 10 cm × 6 cm) at room temperature for 24 hours. Then 50 ml of 4 wt % collagen solutions and 0.2 mg/cm^2 of CCN molecule were uniformly mixed thoroughly for 20 min. Finally, the collagen scaffold with the CCN molecule (COL-CCN) was cast as mentioned above.[45]

Characterization

Fourier Transform Infrared Spectra (FTIR)

Fourier transform infrared (FTIR) measurements were carried out to determine the functional groups present in the prepared COL, CCN and COL-CCN samples. The spectra were measured at a resolution of 4 cm^{-1} in the frequency range of 4000-600 cm^{-1} using ABB 3000 spectrometer with Grams as the operating software. [44]

Proton NMR measurements

Commercially available solvents and reagents were used without further purification. Melting points were determined by capillary tubes and are uncorrected ^{1}H, ^{13}C NMR spectra were obtained in solvent of $CDCl_3$ on a Bruker spectrometer at 400 and 100 MHz, respectively.

ESI-MS Spectra

Mass spectra were recorded by electrospray ionization (ESI), $[M]^+$, $[M^+ +1]$, $[M^+ +2]$ mass peaks were observed. NMR chemical shifts (δ) are relative for tetramethylsilane (TMS, δ=0.00) due to internal standard and it's expressed in parts per million (ppm). Spin multiplicities are shown as s (singlet), d (doublet), t (triplet), m (multiplet). Coupling constants (*J*) were given in hertz.

Thermal analysis

The fabricated collagen scaffold was subjected to thermogravimetric analysis using universal V4.4A TA instruments. 3 mg of the samples was heated at 10 ºC/min at a temperature range of 0-800 ºC using Al_2O_3 crucibles**.** Differential scanning calorimetry (DSC) measurements were taken using the V4.4A Universal instrument from 0ºC to 300ºC at a heating rate of 10ºC /min under nitrogen atmosphere using 3 mg of the samples. [46]

Scanning electron microscope (SEM)

The collagen scaffolds were mounted on brass stub and was gold coated using ion coater (Emitech brand). The surface morphology of the scaffolds was visualized using scanning electron microscope (SEM) (VEGA3 SBH TESCAN) operating at an accelerating voltage of 5– 20 kV.[47]

In vitro degradation studies

All collagen scaffolds were cut into equal dimensions of 2×2cm^2 for *in vitro* degradation studies. All scaffolds were placed in a sealed petriplate containing phosphate buffer solution (PBS, pH value 7.4) with slight agitation at a temperature of 37°C and 100 rpm from 1st week to 4th week. Three samples were recovered at the end of each week and the scaffold were freeze-dried and then weighed. The percentage of degradation was calculated using the following equation.

$$\text{Degradation (\%)} = \left(\frac{W_i - W_f}{W_i}\right) \times 100 \qquad \text{---1}$$

Where W_i is the initial and W_f is the final weight of the scaffold, respectively.[48]

Swelling study

The *in vitro* swelling behavior of the scaffolds were done by immersing square size samples in a phosphate buffer solution (PBS, pH 7.4) at room temperature until the film reached a swelling equilibrium. The swollen weights of the scaffolds were measured at 1, 2, 6, 12, 24, 36, 48, 60 and 72 h after removing the surface wetness by using the filter paper. The equilibrium-swelling ratio was calculated by using the following equation.

$$\text{Swelling (\%)} = \left(\frac{W_i - W_f}{W_i}\right) \times 100 \qquad \text{--- 2}$$

Where W_i is the initial and W_f is the final weight of the scaffold, respectively.[44]

Tensile strength measurement

All the scaffolds were cut into dumb-bell shaped specimens and load-elongation measurement was carried out using a universal testing machine (INSTRON model 1405) according to Vogel at an extension rate of 5 mm/min.[45]

Docking studies of CCN Molecule

A Molecular docking study was carried using Python 2.4 language from https://www.python.org/download/releases/2.4/ and Cygwin from www.cygwin.com, Molecular graphics laboratory (MGL) tools and AutoDock 1.5.6 from http://mgltools.scripps.edu/Support, Chemsketch downloaded from the website with following url http://www.acdlabs.com/resources/freeware/chemsketch.

The compound is subjected to molecular docking using the AUTODOCK 1.5.6 docking program., the X-ray crystal structure of Human 17-Beta-Hydroxysteroid-Dehydrogenase(HBHD) Type 1 C-Terminal Deletion Mutant Complexed with Estradiol and Nadp$^+$ was downloaded from the protein data bank (PDBID: 1A27) and was used for the docking study. The co crystallized ligands (Estradiol and Nadp$^+$) in the protein structure were removed. For the protein structure, polar hydrogen atoms were added, using the ADT version 1.5.6. Further, ADT was used to remove crystal water. We employed the Lamarckian genetic algorithm (LGA) for ligand conformational searching, which is a hybrid of a genetic algorithm and a local search algorithm. The structures were then saved in PDBQT file format, for input into AUTODOCK version 1.5.4. A grid box with dimension of 70X70X70 Å was created using AutoDock Tools. In the AutoGrid procedure, the target enzyme was embedded on a three dimensional grid point

The Ligand 2D structure was drawn using Chemsketch version 12.01. Chem3D Ultra 8.0 was used to convert the 2D structure into 3D and the energy minimized using semi-empirical AM1 method and the ligand were optimized using "Prepare Ligands" in the AutoDock 1.5.6 for docking studies. The optimized ligand molecules were docked into refined using "LigandFit" in the AutoDock. All the structures were saved as a pdb file format for input to AutoDock-Tools (ADT) version 1.5.6. All the ligand structures were then saved in PDBQT file format, for input into AUTODOCK version 1.5.6.

For the AUTODOCK docking calculation, default parameters were used and 50 docked conformations were generated for each compound. AutoDock was run several times to get various docked conformations and used to analyze the predicted docking energy. This reproduced top scoring conformations of 10 falling within the root-mean-square deviation (rmsd) values of 8.99 – 3.84Å from bound X-ray conformation.

Docked ligand conformations were analyzed in terms of energy, hydrogen bonding, and hydrophobic interaction between ligand and receptor protein. Detailed analysis of the ligand–receptor interactions were carried out, and final coordinates of the ligand and receptor were saved as pdb files. From the docking scores, the free energy of binding (FEB) was calculated. The docking poses were ranked according to their docking scores and both the ranked list of docked ligands and their corresponding binding poses.

Flow Cytometry by Annexin V conjugate with FITC

Flow cytometry study was carried out using Annexin V and Propidium Iodide staining. About 5 x 10^4 cells/mL of MCF-7 cells and Hep2 cells were seeded on to 6 wells Microtitre plates. After 48h, the medium was discarded and fresh medium was added with IC_{50} value concentration. The cells were monitored with fixation to assess the morphological changes (apoptosis) induced by the compound CCN (4a).

The apoptosis was also assessed by staining with Annexin V- FITC. This assay is based on the affinity between Annexin V- FITC towards Phosphatidyl Serine (PS), which translocates from the inner surface of PM to the cell surface during apoptosis. Annexin V is not an absolute marker for apoptosis. Therefore, another vital dye, Propidium Iodide (PI) was used in conjugation with Annexin V-FITC. Cells were washed with PBS for several times followed by

trypsinization of cells for 30 seconds. Cells were dissolved in 500 µL of PBS. To which 100 µL of 1X binding buffer was added to the cell suspension. Then 5 µL of Annexin V- FITC conjugate and 10 µL of Propidium Iodide solution were added. The vials were incubated at room temperature for 10 min in dark. Flow Cytometry was determined immediately using a Flow Cytometer (BD. Sasc. Jazz Trademark, US).

In vitro cytotoxicity assay of CCN Molecule

The cytotoxic effect of compounds against MCF-7, Hep-2 and Vero cancer cell lines was determined by using 3-(4, 5 dimethythiazol-2-yl)-2,5-diphenyl tetrazolium bromide (MTT) and compared with untreated controls were shown in Figure 2 .[50] For the screening experiment, the cells were seeded in 96-well plates in 100µL of medium containing 5% FBS, at plating density10,000 cells/well and incubated at 37°C in a humidified atmosphere of 5 % CO_2 for 48 h prior to addition of compounds. After 48h, compounds at various concentrations was added and incubated at 37°C in a humidified atmosphere of 5 % CO_2 for 48 h. Triplicate was maintained and the medium containing without the sample served as control.

After 48 h, 50 µL of MTT (5 mg/mL) in triple distilled water was added to each well and incubated at 37°C for 4h. The medium with MTT was then flicked off and the formed formazan crystals were solubilised in 100 µL of DMSO and then measured the absorbance at 570 nm using Universal Microplate Reader.

$$\text{Cell inhibition (\%)} = \frac{100 - \text{Absorbance (Sample)}}{\text{Absorbance (control)}} \times 100 \text{ --- 3}$$

In vitro biocompatibility of the COL-CCN scaffold

The cell viability assay and cell attachment and proliferation assay for COL-CCN scaffold were done using of the NIH 3T3 fibroblast cell line. The cells were grown on the scaffolds placed in 24-well plates (Corning, NY) and maintained in DMEM with 10% fetal calf serum supplemented with penicillin (120 units per mL), streptomycin (75 mg/mL^{-1}), gentamycin (160 mg/mL^{-1}), and amphotericin B (3 mg/mL^{-1}) at 37°C at a density of 5×10^4 cells/mL and then incubated for 24 h in a humidified atmosphere of 5 % CO_2.

Cell viability of the COL-CCN scaffolds was done using MTT assay. Cells cultured in blank wells were used as a control. After 48 h, the culture medium was replaced with a serum-free medium containing 10 µL of MTT and incubated at 37°C for 4 h in a humidified atmosphere of 5 % CO_2. The medium was aspirated and then 500 µL/well of dimethylsulfoxide (DMSO) was added to dissolve the formazan needles and the absorbance of the dissolved solution was measured at 570 nm using Universal Microplate Reader.[48]

Cell adhesion and proliferation assay of COL-CCN scaffold

The cell attachment and proliferation of NIH 3T3 fibroblast were quantified by a live/dead assay. The live/dead assay was done at regular time intervals (6, 12, 24, 48 hours), the medium was removed and washed with PBS, to which Calcein AM solution (4 µM; 500 µl) was added and incubated for 30 min. The plates with scaffold were washed with PBS and viewed at fluorescence microscope with a blue filter (Euromex, Holland).[51]

Minimum inhibitory concentration (MIC) of the synthesized compound (4a-4j)

The *in vitro* minimum inhibitory concentration (MIC) of the compound against human pathogens was determined by the method of the National Committee for Clinical Laboratory (NCCLS)[52]. The standard antibiotics, Streptomycin and Fluconazole triclosan were used as controls.

Antimicrobial activity of the synthesized compound (4a-4j)

The parent and synthesized compounds were initially screened for their antimicrobial activity against the Gram positive bacterium, Methicillin resistant *Staphylococcus aureus* (MRSA), Gram negative bacterium, *Pseudomonas aeruginosa* MTCC 201, *Escherichia coli*, *Salmonella typhi* and a yeast strain, Fluconazole resistant *Candida albicans* (FRCA). The well diffusion assay was carried out to determine the antimicrobial activity.[53] For the well diffusion assay, 17 h old bacterial cultures were inoculated over the agar surface of Mueller Hinton agar plates using sterile cotton swabs. After 10 min, wells were cut using a cork borer and each well was loaded with 100 µl of compound from 1 mg/ml stock (100 µg/well) along with DMSO control. The plates were incubated at 37°C for 24 h.

Antimicrobial activity of the COL-CCN scaffold

In this study, one Gram positive bacteria *Staphylococcus aureus* (ATCC 11632) and one Gram negative bacteria *Escherichia coli* (ATCC 10536). All bacterial cultures were sub-cultured and maintained aseptically. The antimicrobial activity of the scaffold was evaluated using modified agar well diffusion method. About 100 µL [10^5 CFU (colony forming units)] of each bacterial culture was spread on the agar surface (Muller-Hinton agars) using a sterile glass spreader. The COL and COL-CCN scaffold were placed on the agar and they were kept in a refrigerator for 20 min for diffusion. Then, the plates were incubated for 24 h at 37 ºC. The antibacterial activity was evaluated by measuring the zone of inhibition against the test organism.[54]

Statistical analysis

All the experiments were conducted in triplicate. Results are presented as mean ± S.D. (n = 3). ANOVA (analysis of variance) and student's t-test was done to determine the significant differences among the groups. The observed differences were statistically significant when $p < 0.05$.

Results and discussion

Chemistry

This is a novel approach to introduce the combination of coumarin and chromen group which are highly specified compounds for biologically essential heterocyclic moiety. In the first analysis, 4-Hydroxycoumarin, Chromene-3-carbaldehyde and N-Methyl-1-1(methylthio)-2-nitroethylene-1-amine (NMSM) were selected as an initial substrate to optimize the condition of the reaction. First, the above given three component reaction was carried out at room temperature in the presence of ethanol, there was no product formation even after one day. Further we tried to optimize the reaction condition with different catalyst and various solvents. Through our observation the combination of TEA (0.1 eq.), EtOH, has given major conversion of reaction with good yield and short reaction time. We revealed a chemo and regioselective synthesis of 2-(methylamino)-3-nitro-4-(4-oxo-4H-chromen-3-yl)pyrano [3,2 c]chromen-5(4H)-one by one pot three component coupling of NMSM(N-Methyl-1-1(methylthio)-2-nitroethylene-1-amine), Chromene-3-carbaldehyde, and 4-Hydroxycoumarin (Scheme1). The reactions were completed within 2-4 hours and pure products could be isolated simply by filtration and the reaction optimizations were given in Table 1.

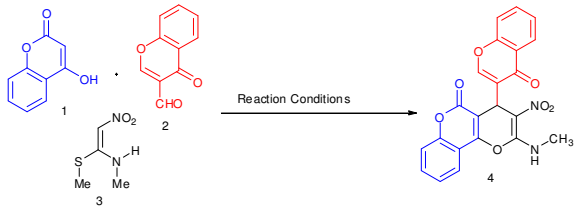

Scheme 1 synthesis of 2-(methylamino)-3-nitro-4-(4-oxo-4H-chromen-3-yl)pyrano[3,2-c]chromen-5(4H)-one.

Table 1 Optimization of reaction condition for the synthesis of 2-(methylamino)-3-nitro-4-(4-oxo-4H-chromen-3-yl)pyrano[3,2-c]chromen-5(4H)-one[a]

Entry	Reaction	Condition	Time	Yield[b] (%)
1	No Catalyst	EtOH	24(h)	_c
2	Piperidine (0.1 eq.)	EtOH	8(h)	57
3	DBU (0.1eq)	EtOH	10(h)	21
4	DABCO (0.1eq.)	EtOH	24(h)	30
5	p-TSA (0.1 eq.)	EtOH	6(h)	31
6	L-Proline (0.1 eq.)	EtOH	7(h)	43
7	$InCl_3$ (0.1 eq.)	EtOH	4(h)	36
8	CAN (0.1 eq.)	EtOH	15(h)	_c
9	TEA (0.1 eq.)	EtOH	4(h)	83
10	TEA (0.2 eq.)	EtOH	8(h)	75
11	$Cu(TfO)_3$ (0.1 eq.)	EtOH	7(h)	25
12	TEA (0.1 eq.)	MeOH	5(h)	65
13	TEA (0.1 eq.)	CH_3CN	8(h)	45
14	TEA (0.1 eq.)	Toluene	24(h)	_c

[a]All reaction was performed at r.t.
[b]Yield of the products after recrysatlzation.
[c]No reaction.

The structure of all novel synthesized products was confirmed by spectral data of ^{1}H NMR, ^{13}C NMR and FTIR, ESI-MS (Given as Electronic Supplementary Information in S1 (^{1}H ,^{13}C NMR and ESI-MS Spectrum of all compounds were given as supplementary information in S1) analysis. The mass data of products were displayed molecular ion peak at *m/z* values. Further the single crystal X-ray diffraction studies exactly confirmed the structure of product 4c[69] Fig.1

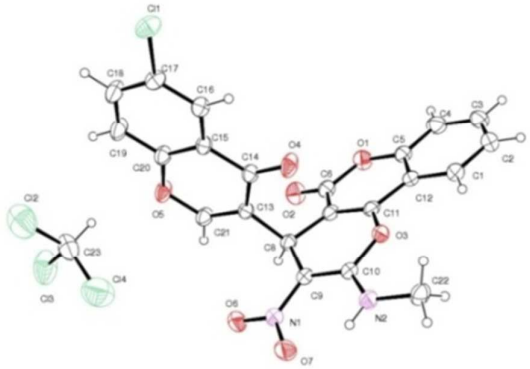

Figure 1 ORTEP diagram of compound 4c

Based on the reaction, the Table 2 and Table 3 exhibits the various derivatives and different percentage of the yield of the product. The plausible mechanism is proposed to formation of 2-(methylamino)-3-nitro-4-(4-oxo-4H-chromen-3-yl)pyrano[3,2-c]chromen-5(4H)-one

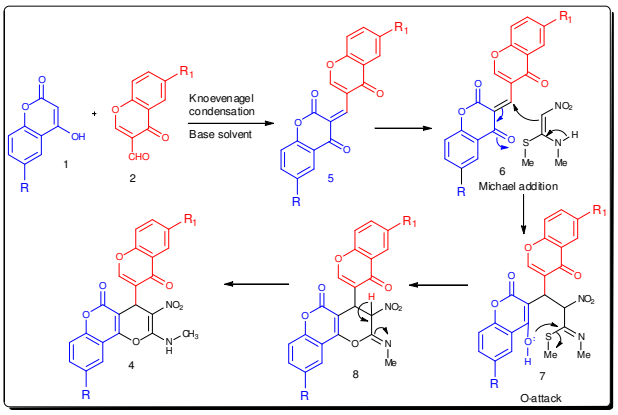

Scheme-2; Plausible reaction mechanism for the formation of 2-(methylamino)-3-nitro-4-(4-oxo-4H-chromen-3-yl)pyrano[3,2-c]chromen-5(4H)-one **4.**

4 (Scheme 1). Initially the knoevenagel condensation reaction between 4-Hydroxycoumarin reacts with Chromene-3-carbaldehyde to give a coumarin chromen adduct **5,** which act as Michael acceptor. The adduct **5** immediately undergoes Michael type addition with NMSM **3** to generate the intermediate **6.** The intermediate **6** undergoes intramoleculear O-cyclization reaction to obtain the product by the elimination of MeSH. Based on the reaction mechanism, O-cyclization process has been fevered for chemo and regioselective of the products (Scheme 2)

The main favour of this multicomponent reaction was a great advantage as the product was obtained in excellent purity by simple filtration, which generates this procedure facile, practical and accelerated to expeditious. The purity of the target molecule was sufficient for further implementation of collagen scaffold.

Biological applications

Antimicrobial activity of the synthesized compound (4a-4j)

The Susceptibility was assessed on the basis of the diameter of the zone of inhibition (ZOI) against the microbes and the results were presented in Table 4. The compound showed activity for gram positive and gram negative, but there was no activity against yeast. Based on the results, it was clearly exhibited among the synthesized compound that compound 4a (CCN) showed significant antibacterial action against both gram positive and gram negative bacterium[53].

Table 2 Synthesis of 2-(methylamino)-3-nitro-4-(4-oxo-4H-chromen-3-yl)pyrano[3,2-c]chromen-5(4H)-one 4a-4j.

Entry	Product	R	R_1	Time	Yield[b] (%)
1	4a	H	H	2.0	83
2	4b	H	6-Me	3.0	81
3	4c	H	6-Cl	2.5	75
4	4d	H	7-F	3.0	82
5	4e	H	6-F	3.0	83
6	4f	H	6, 8-Cl	2.0	80
7	4g	H	6-Br	2.0	79
8	4h	6-Me	6-Br	5.0	82
9	4i	6-Me	6-Me	3.5	75
10	4j	6-Me	6-Cl_2	3.0	81

[a]Yield after rectystallization.

Table 3 Synthesis of variety of pyrano[3,2-c]chromen-5(4H)-one derivatives

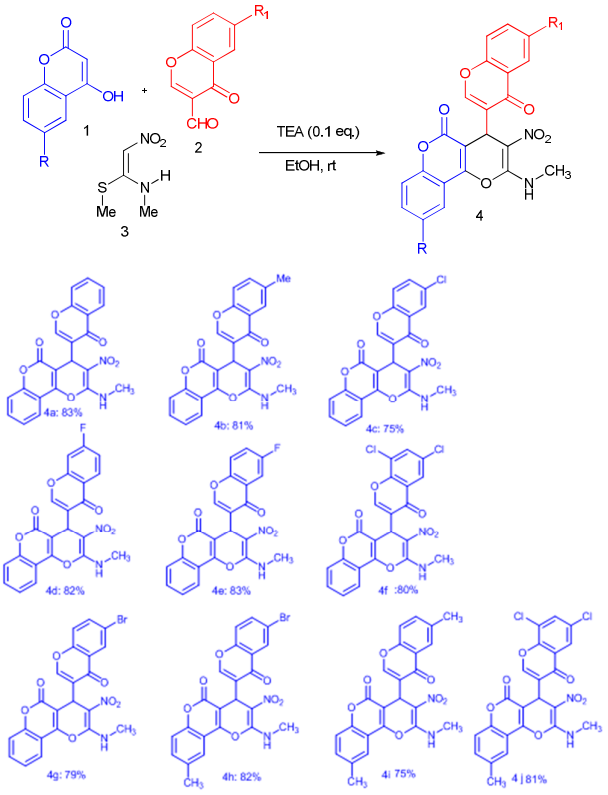

Table 4 Antimicrobial activity of synthesized compound against microbes

Compound	Zone of inhibition (mm)				
	Gram +ve bacterium	Gram-ve bacterium			Yeast strain
	MRSA	*P. aeruginosa*	*S. typhi*	*E. coli*	*FRCA*
4a	8	10	10	8	N
4b	4	N	N	N	N
4c	4	4	4	3	N
4d	3	3	3	3	N
4e	4	N	N	N	N
4f	3	N	3	N	N
4g	5	5	5	4	N
4h	5	4	4	4	N
4i	4	N	N	N	N
4j	4	N	N	N	N
PC	N	10	N	N	N
NC	N	N	N	N	N

Streptomycin 30µg for MRSA, P. aeruginosa, S. typhi and E. coli
Fluconazole 30µg for the FRCA.
Negative Control: 10% DMSO.
N: No inhibition.

Table 5 Minimum inhibitory concentration of the compounds against microbes

Compound	MIC (µg/ml)				
	Gram +ve bacterium	Gram -ve bacterium			Yeast strain
	MRSA	*P. aeruginosa*	*S. typhi*	*E. coli*	*FRCA*
4a	62.5	15.6	15.6	62.5	ND
4b	250	ND	ND	ND	ND
4c	250	125	125	125	ND
4d	250	250	250	250	ND
4e	125	ND	ND	ND	ND
4f	500	ND	500	ND	ND
4g	250	250	250	250	ND
4h	500	250	250	250	ND
4i	500	ND	ND	ND	ND
4j	250	ND	ND	ND	ND
PC	ND	15.6	ND	ND	ND
NC	ND	ND	ND	ND	ND

ND: Not determined as they did not show antimicrobial activity in the well diffusion assay.

Since the activity of the synthesized compounds was not as effective as compound (CCN) anticancer study was carried out in compound 4a.

Minimum inhibitory concentration (MIC) of the synthesized compound (4a-4j)

The MIC values are summarized in Table 5 for the compounds (4a-4j). When comparing all the compounds with gram positive, gram negative and yeast strain, the compound 4a (CCN) showed consistently a better result with an effective growth inhibitor against microbes. Further the nature of the CCN against the microbes contributed to the antimicrobial potency in the COL-CCN scaffold[52].

In vitro cytotoxicity assay of CCN Molecule

The IC_{50} values of CCN molecule against the MCF-7, Hep-2 and Vero cancer cell lines were given in Table 6. It was seen that CCN concentrations against all cells showed suppressed cell growth and exhibited the highest inhibitory effect on its IC_{50} values and that was confirmed by the Apoptotic potential against MCF-7 and Hep-2 cancer cell lines[50]. Apoptotic potential of compound on Hep-2, MCF-7 and Vero cell lines was depicted in Figure 2 (a)-(f).

Flow Cytometry by Annexin V conjugate with FITC

Staining with Annexin V- FITC conjugate and Propidium Iodide showed the amount of cells in apoptotic stage, late apoptotic stage, live stage and necrotic cells has been depicted in Figure 3. Based on the IC_{50} CCN (4a) 53 µg and 54 µg concentration were used to treat Hep2 and MCF-7 cell line. The Hep2 Cells showed 58.36% of necrotic cells 13.69% of late apoptotic cells, 1.22% early apoptotic cells and 13.23% of live cells. In MCF-7 cell line, 78.99% of necrotic cells, 11.86% of late apoptotic cells, 0.68% of early apoptotic cells and 2.84% of live cells were observed.

Table 6 IC_{50} values of compound on the growth against cancer cell lines

Compound	IC_{50} (µg/ml)		
	Hep-2	MCF-7	Vero Cells
CCN (4a)	5.3	5.4	68.4

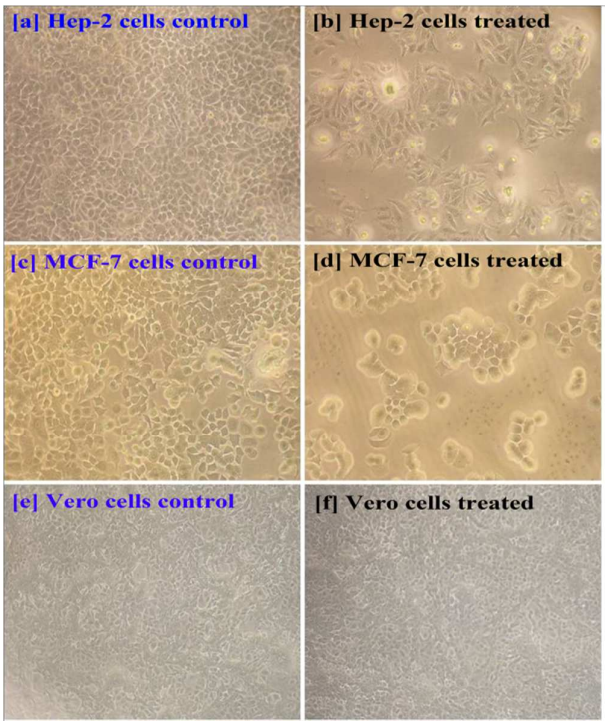

Figure 2 (a) –(f) Microscopic images of control and treated Hep-2, MCF-7 and Vero cells

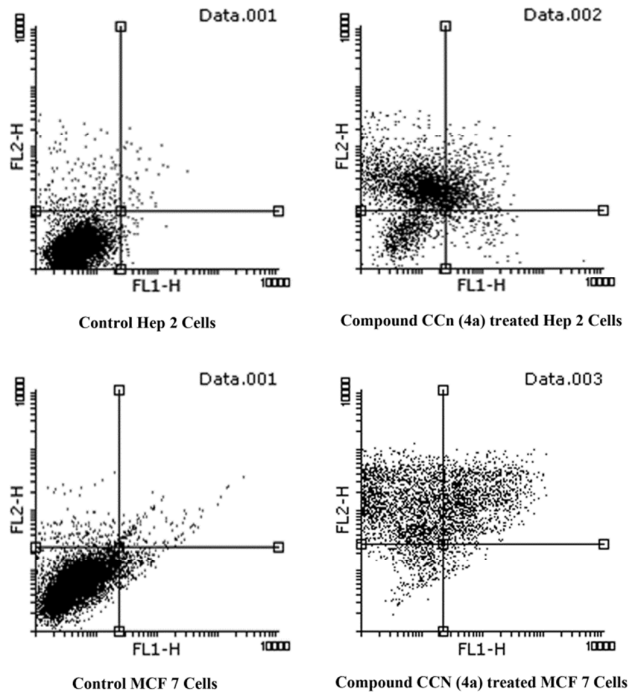

Figure 3 Flow cytometry study for CCN (4a) molecule by Annexin V conjugate with FITC

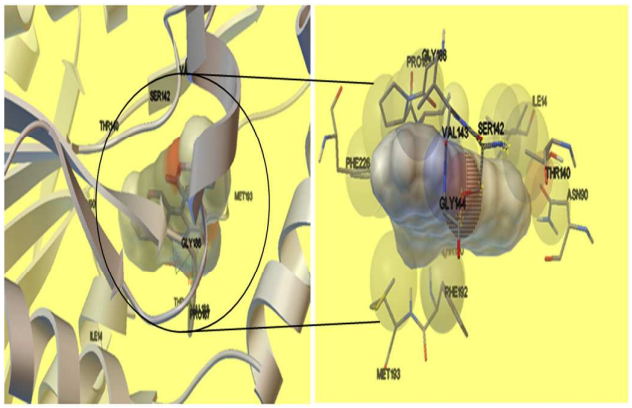

Figure 4 Molecular docking of active compound (CCN) (FEB= -12.42 Kcal/mol^{-1}) with protein (PDBID: 1A27) with the ligand

Docking studies of CCN Molecule

The results revealed that compound(CCN) was most active with a calculated binding energy of -12.42 kcal/mol. The binding interactions of these compounds were shown in Figure 4. We revealed the catalytic efficiency Human 17-Beta-Hydroxysteroid-Dehydrogenase (HBHD) Type 1 C-Terminal Deletion Mutant Complexed with Estradiol and Nadp+ (PDBID: 1A27) with the ligand. The active compound (CCN) binds with HBHD receptor and the result of binding energy value -12.42 Kcal/mol^{-1}. Compound interacts with only two amino acids, namely, THR -190 and VAL-188 through two hydrogen bonds with HBHD receptor.

Characterization of the collagen scaffold with CCN molecule

Fourier Transform Infrared Spectra (FTIR)

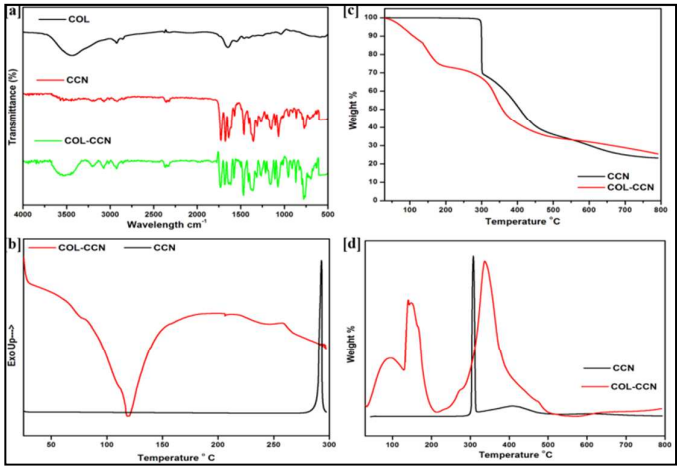

Figure 5 (a) Fourier Transform Infrared spectra (FTIR) (b) Differential scanning calorimetry (DSC) (c) Thermogravimetric analysis (TGA) and (d) Differential thermal analysis (DTA) curves of CCN and COL-CCN scaffolds

Table 7 Thermal properties of COL and COL-CCN scaffolds

Sample Name	$T_{-5\%}$ (°C)	T_{max1} (°C)	T_{max2} (°C)	T_d (°C)	T_m (°C)	ΔH_m (J/g)	ΔH_d (J/g)
CCN	277.1	299.6	-	-	292.7	494.1	-
COL-CCN	106.9	147.1	336.1	68.3	-118.8	-371.5	-2.6

The Fourier Transform Infrared (FTIR) spectra of the COL, CCN and COL-CCN scaffold was depicted in Figure 5(a). The main structural protein, collagen exhibits amide A, amide I, II and III absorption band at 3435 (N–H stretching vibration), 1635, 1556 and 1261 cm^{-1} respectively [43]. The IR spectrum of compound CCN showed a peak at 3220 cm^{-1}, which reported the presence of -NH functional group, respectively. The stretching bands at 1730 cm^{-1} confirmed the presence of carbonyl (C=O) group. The stretching bands at 1360cm^{-1} corresponds to the C-N group. The peak at 1400-1600 cm^{-1} stretching band which has revealed the presence of aromatic (C=C) group. The CCN impregnated scaffold spectrum showed the presence of N–H functional group at 3442 cm^{-1} and the carbonyl group band at 1733 cm^{-1} indicates the inconclusiveness of CCN molecules with collagen.[55, 56]

Thermal analysis

The TGA thermogram of the CCN and COL-CCN was depicted in Figure 5(c) and (d). The loss of moisture in the COL-CCN occurred over a temperature range from 90°C- 110°C and related to initial weight loss of the scaffold. The first weight loss corresponds to the increase in the composition of collagen, which was apparent from the $T_{-5\%}$ values listed in Table 7. DTA of the both CCN and collagen blended CCN was shown in Figure 5(d). Two Tmax values were observed for COL-CCN scaffold with degradation of collagen and CCN molecule respectively. The Tmax value at 299.6°C corresponds to the degradation of CCN molecule alone. The Tmax1 value corresponds to decomposition of CCN molecule and further impregnation of CCN into collage does not affect the thermal decomposition of triple helix in collagen scaffold.[57-59]

Figure 5(b) represents the DSC thermogram of CCN molecule and COL-CCN scaffold. Since the triple helix structure of the collagen gets disturbed by the breaking of hydrogen bonds with rearrangement of the triple helix configuration which involves a characteristic endothermic transition often termed as denaturation temperature (T_D) and corresponding melting heat of the triple helix reflects with denaturation enthalpy (ΔH_D). The thermal denaturation of the collagen in the COL-CCN scaffold was observed at 68.3°C as first endothermic transition. The decrease in the T_m and ΔH_m was found when compared with the CCN molecule alone. Thus, increase in the composition of the collagen in COL-CCN corresponds to the decreased thermal properties of CCN. However the CCN molecule makes the scaffold thermally stable due to the interaction of both collagen and CCN molecules.[59,60] The thermal properties of the scaffold and the molecule were listed in Table 7

Proton NMR spectrum

Proton NMR spectrum **1(CCN)** shown the compound and spectrum **2(COL-CCN)** shown the synthetic molecule in the collagen scaffold (Figure 6). ^{1}H NMR spectrum of **2**-(methylamino)-3-nitro-4-(4-oxo-4H-chromen-3-yl)pyrano[3,2-c]chromen-5(4H)-one **(1)** has displayed chemical shifts at δ 8.39 (s, 1H), 8.00 (dd, *J* = 8.0, 1.5 Hz, 1H), 7.91 (dd, *J* = 7.9, 1.3 Hz, 1H), 7.62 (dddd, *J* = 7.5, 6.2, 4.5, 1.6 Hz, 2H), 7.48 – 7.29 (m, 4H), these values have given presence of aromatic protons and the chiral proton of aldehyde shows a singlet at 5.03 ppm. By the by the presence of synthetic compound in the collagen **(2)** scaffold has given peak at 5.89 ppm for the chiral proton in difference of shielding region. However, COL-CCN has important chemical shift values at the aromatic region as identical for the conformation of fusion.

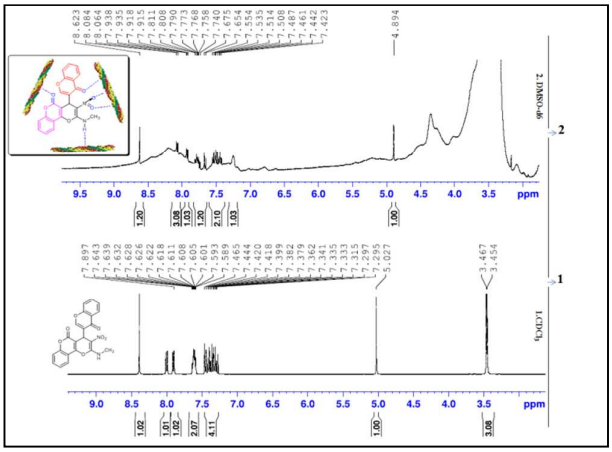

Figure 6 Proton NMR spectrum of CCN molecule and COL-CCN scaffold

Scanning Electron Microscopy

The morphology of the scaffold was observed in the scanning electron microscopy as depicted in Figure 7(a) and (b). The collagen scaffold showed a smooth uniform morphology through the surface with minute pores. The COL-CCN scaffold showed uniform coarse surface due to the presence of CCN molecule. Collagen being biocompatible with cell recognition sites, supports the growth of fibroblast. Similarly CCN impregnated collagen scaffold with coarse surface will aid the cell attachment.[60,61]

Swelling study

The tissue engineering material, should enhance oxygen permeability and the capacity to hold large amount of exudates. Figure 8(a) depicted the swelling behavior of the scaffolds. It was found that COL scaffold exhibits maximum swelling from the initial hour. The COL-CCN attains a constant swelling rate with a strong interaction between the collagen and CCN molecule through 24 h. The presence of collagen in the scaffold makes the material to exhibit better swelling rate, which signifies that the scaffold was partially hydrophilic in nature.[44, 63]

In vitro degradation studies

Figure 8(b) shows the *in vitro* degradation profile of the COL and COL-CCN scaffolds. The profound swelling of COL scaffold started during the beginning of the first week. The COL scaffold showed an excess fragmentation when compared to that of the COL-CCN scaffold. The COL-CCN scaffold exhibits a negligible degradation up to the fourth week. The presence of CCN makes the scaffold more stable with a strong interaction with the collagen.[62] Hence, the CCN composition in the collagen matrix provides more stability to make the scaffold more suitable for tissue engineering.

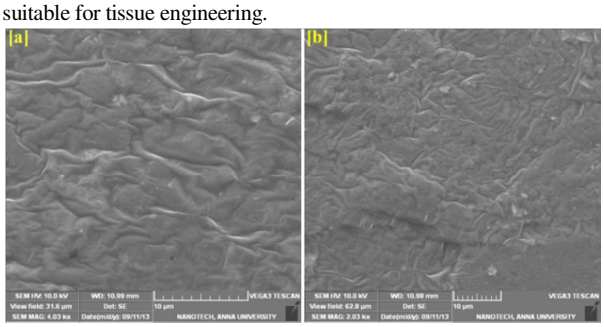

Figure 7 SEM images of (a) COL (b) COL-CCN scaffolds

Table 8 Tensile properties of COL and COL-CCN scaffold

Scaffold name	Tensile strength (MPa)	Elongation at break (%)	Extension at maximum load (mm)	Young's Modulus (MPa)
COL	4.1±0.9	12.2±0.8	3.35±0.1	1.2±0.27
COL-CCN	3.6±0.3	13.9±1.1	2.83±0.2	1.3±0.23

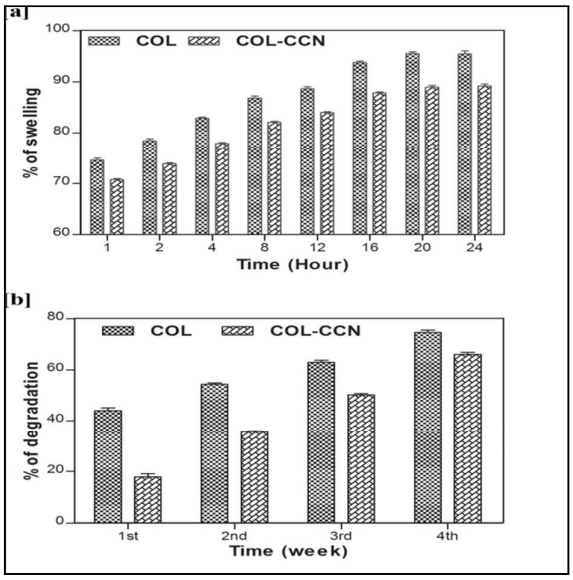

Figure 8 (a) Swelling study behavior and (b) In vitro degradation studies of COL and COL-CCN scaffolds

Tensile strength

The wound dressing scaffold should encompass better mechanical property to ensure a easy handling by the physician on the wound surface. In this view, tensile strength of COL and COL-CCN scaffold were given in Table 8. The CCN molecule impregnated scaffold exhibits a slight increase in young's modulus of 1.3±0.23 MPa when compared to that of COL scaffold. The CCN was impregnated not only to enhance the collagen property, but also to prevent bacterial infection at the wound site.[54, 64]

***In vitro* studies of the collagen scaffold with CCN molecule**

***In vitro* biocompatibility, Cell adhesion and proliferation of the scaffold**

The material should possess cell adherence and proliferation property before it has to be applied in vivo application. The present work exhibits the cell adherence and proliferation of the COL-CCN scaffold assessed using NIH 3T3 fibroblast cells. Figure 9 shows the fluorescence image of the cells at different time intervals. When live cells were stained with calcein fluorescent probe, the non fluorescent calcein AM converted to green fluorescent calcein after the ester hydrolysis of intercellular esterases. There were no remarkable difference in fluorescence intensity between the COL-CCN scaffold and the control. The scaffold with CCN molecule increased in cell viability and has not showed any negative impact on it.[65, 66]

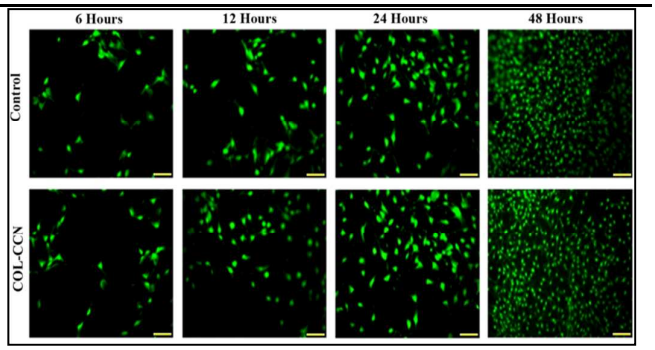

Figure 9 *In vitro* fluorescence images of NIH 3T3 fibroblast cells on adherence and proliferation on COL-CCN in comparison with control at various time intervals of 6, 12, 24 and 48 hours. Blue filter was used for fluorescence excitation and emission. The scale bar measures 10 µm.

To estimate the percentage of cell viability, *in vitro* biocompatibility studies of NIH 3T3 fibroblast were performed with MTT assay (Figure 10). The cells are widespread, with no obvious cell death or undesirable effects noticed in treated wells . The fluorescent image and MTT assay of the COL-CCN scaffold were found to be biocompatible with cellular adhesion and proliferation. Both the scaffold showed relatively comparable change with cell viability. More than 92% of cell viability was observed in both scaffolds.

The increase in the biocompatibility of the scaffold was due to the presence of the biomimetic nature of the collagen with affinity toward fibroblast attraction in production of extracellular matrix.[44, 67, 68]

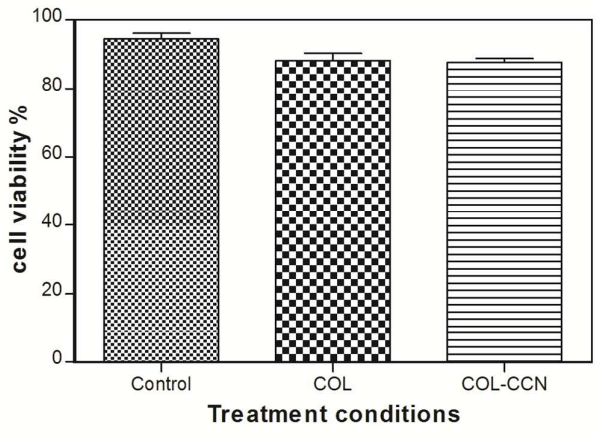

Figure 10 Cell viability assessment based on MTT assay quantification of NIH 3T3 fibroblasts on the scaffolds

Antimicrobial activity of the scaffold

The antimicrobial activity of CCN impregnated collagen scaffold was evaluated selective against two bacterial strains (Figure 11). COL scaffold with 0.2 mg/20 x 10 mm2 concentration of CCN molecule showed gradual diffuse of CCN from the COL scaffold against *Staphylococcus aureus* and *Escherichia coli* with clear zone formation, which implies that CCN exhibited admirable bactericidal activity. The COL-CCN scaffold material proves to be prospective biomaterial that will prevent infection around the wounded region. [54, 45]

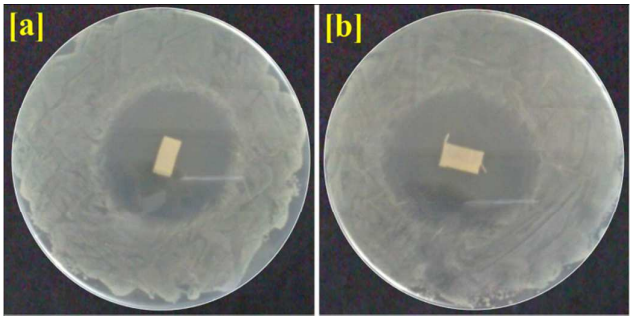

Figure 11 Antimicrobial activity of the COL-CCN scaffolds using: (a) Staphylococcus aureus, (b) Escherichia coli

Conclusion

In the present work, we have attempted to synthesize and characterized various chromen and pyrano chromen-5-one derivatives with excellent versatile biological applications. The advantage of the CCN moiety impregnated over the collagen scaffold has increased the therapeutic values. However, a synthetic molecule generated multi position interactions by hydrogen bonding with the collagen scaffold. In our observation studies, we confirmed that the nature of scaffold did not show any structural changes after impregnation of CCN molecule. It exhibited good thermal, mechanical and swelling property. Further, the COL-CCN scaffold revealed with increased antimicrobial activity to prevent against microbes and NIH 3T3 fibroblast showed excellent *in vitro* biocompatibility. Hence the development of collagen scaffold with novel CCN molecule achieved as a suitable biomaterial in the field of tissue engineering and biomedical application.

Experimental data for synthesized molecules (4a-4j)

2-(methylamino)-3-nitro-4-(4-oxo-4H-chromen-3-yl)pyrano[3,2-c]chromen-5(4H)-one(4a)

White solid; mp 280-281°C. ^{1}H NMR (400 MHz, $CDCl_3$) δ 10.54 (d, *J* = 4.8 Hz, 1H), 8.39 (s, 1H), 8.00 (dd, *J* = 8.0, 1.5 Hz, 1H), 7.91 (dd, *J* = 7.9, 1.3 Hz, 1H), 7.62 (dddd, *J* = 7.5, 6.2, 4.5, 1.6 Hz, 2H), 7.48 – 7.29 (m, 4H), 5.03 (s, 1H), 3.46 (d, *J* = 5.3 Hz, 3H). ^{13}C NMR (100 MHz, $CDCl_3$) δ 177.27, 160.02, 158.99, 157.06, 156.17, 153.67, 152.79, 133.67, 132.98, 125.19, 125.14, 124.73, 122.38, 118.37, 117.10, 112.83, 105.79, 103.46, 32.51, 28.55. IR (KBr, cm^{-1}): 3220, 1730, 1712, 1676, 1570, 1454, 1360, 1126, 1066. ESI-MS: *m/z* 419 [M^+ +1]. Anal. Calcd for $C_{22}H_{14}N_2O_7$: C, 63.16; H, 3.37; N, 6.70; O, 26.77. Found: C, 63.01; H, 3.61; N, 6.68; O, 26.71. HRMS (ESI) calc. $C_{22}H_{15}N_2O_7$ for [M^++H] 419.0879, found: 419.0876.

4-(6-methyl-4-oxo-4H-chromen-3-yl)-2-(methylamino)-3-nitropyrano[3,2-c]chromen-5(4H)- one(4b)

White solid; mp 280-282°C. ^{1}H NMR (400 MHz, $CDCl_3$) δ 10.54 (d, *J* = 4.8 Hz, 1H), 8.38 (s, 1H), 7.91 (dd, *J* = 7.9, 1.4 Hz, 1H), 7.80 (d, *J* = 1.2 Hz, 1H), 7.66 – 7.57 (m, 1H), 7.47 – 7.33 (m, 4H), 5.03 (s, 1H), 3.46 (d, *J* = 5.3 Hz, 3H), 2.36 (s, 3H). ^{13}C NMR (100 MHz, $CDCl_3$) δ 177.41, 160.04, 159.03, 156.98, 154.48, 153.65, 152.81, 135.19, 134.94, 132.94, 124.70, 124.43, 124.01, 122.36, 118.42, 118.12, 117.11, 112.86, 105.86, 103.52, 32.47, 28.52, 20.86. IR (KBr, cm^{-1}): 3233, 1788, 1634, 1512, 1330, 1212, 988, 950, 832, 790, 612. . ESI-MS: *m/z* 432 [M^+ +1]. Anal. Calcd for $C_{23}H_{16}N_2O_7$: C, 63.89; H, 3.73; N, 6.48; O, 25.90. Found: C, 63.74; H, 3.95; N, 6.46; O, 25.84. HRMS (ESI) calc. C23H16N2NaO7 for [M^++Na] 455.0855, found: 455.0854.

4-(6-chloro-4-oxo-4H-chromen-3-yl)-2-(methylamino)-3-nitropyrano[3,2-c]chromen-5(4H)-one(4c)

White solid; mp 282-283°C. ^{1}H NMR (400 MHz, $CDCl_3$) δ 10.52 (d, *J* = 5.1 Hz, 1H), 8.40 (s, 1H), 7.99 (d, *J* = 2.5 Hz, 1H), 7.92 (dd, *J* = 8.0, 1.4 Hz, 1H), 7.67 – 7.60 (m, 1H), 7.57 (dd, *J* = 9.0, 2.6 Hz, 1H), 7.47 – 7.34 (m, 3H), 5.05 (s, 1H), 3.47 (d, *J* = 5.3 Hz, 3H) ^{13}C NMR (100 MHz, $CDCl_3$) δ 176.19, 158.98, 157.20, 154.50, 153.80, 152.84, 133.91, 133.09, 131.21, 125.27, 124.80, 124.70, 122.35, 120.10, 118.84, 117.19, 112.77, 103.21, 32.43, 28.54. IR (KBr, cm^{-1}): 3328, 1760, 1606, 1568, 1319, 814, 760, 638. ESI-MS: *m/z* 452 [M^++Z]. Anal. Calcd for $C_{22}H_{13}ClN_2O_7$: C, 58.36; H, 2.89; Cl, 7.83; N, 6.19; O, 24.73. Found: C, 58.36; H, 2.89; Cl, 7.83; N, 6.19; O, 24.73. HRMS (ESI) calc. $C_{22}H_{14}ClN_2O_7$ for [M^++H] 453.0490, found: 453.0493.

4-(7-fluoro-4-oxo-4H-chromen-3-yl)-2-(methylamino)-3-nitropyrano[3,2-c]chromen-5(4H)-one (4d)

White solid; mp 281-282°C. ^{1}H NMR (400 MHz, $CDCl_3$) δ 10.53 (d, *J* = 4.8 Hz, 1H), 8.41 (s, 1H), 7.92 (dd, *J* = 7.9, 1.3 Hz, 1H), 7.63 (td, *J* = 8.5, 2.2 Hz, 2H), 7.52 – 7.32 (m, 4H), 5.05 (s, 1H), 3.47 (d, *J* = 5.2 Hz, 3H). ^{13}C NMR (100 MHz, $CDCl_3$) δ 176.54, 160.70, 160.03, 158.98, 158.24, 157.26, 153.76, 152.82, 152.44, 133.08, 125.56, 125.48, 124.80, 122.37, 122.12, 121.87, 120.57, 120.49, 118.16, 117.17, 112.78, 110.14, 109.91, 105.65, 103.28, 32.41, 28.56. IR (KBr, cm^{-1}): 3220, 1733, 1710, 1683, 1576, 1462, 1332, 1265, 1165, 1555, 1133, 1105, 1066, 980. ESI-MS: *m/z* 437 [M^+ +1]. Anal. Calcd for $C_{22}H_{13}FN_2O_7$: C, 60.56; H, 3.00; F, 4.35; N, 6.42; O, 25.67. Found: C, 60.42; H, 3.23; F, 4.34; N, 6.41; O, 25.61. HRMS (ESI) calc. for $C_{22}H_{13}FN_2NaO_7$ [M^++Na] 459.0604, found: 459.0612.

4-(6-fluoro-4-oxo-4H-chromen-3-yl)-2-(methylamino)-3-nitropyrano[3,2-c]chromen-5(4H)-one (4e)

White solid; mp 280-281°C. ^{1}H NMR (400 MHz, $CDCl_3$) δ 10.53 (d, *J* = 4.2 Hz, 1H), 8.37 (s, 1H), 8.02 (dd, *J* = 8.9, 6.2 Hz, 1H), 7.91 (d, *J* = 7.9 Hz, 1H), 7.63 (t, *J* = 7.2 Hz, 1H), 7.46 – 7.33 (m, 2H), 7.14 (dd, *J* = 9.0, 2.1 Hz, 1H), 7.11 – 7.00 (m, 1H), 5.04 (s, 1H), 3.46 (d, *J* = 5.2 Hz, 3H). ^{13}C NMR (100 MHz, $CDCl_3$) δ 176.41, 164.27, 160.01, 158.99, 157.19, 153.75, 152.84, 133.06, 127.80, 127.70, 124.77, 122.36, 118.81, 117.18, 114.25, 114.02, 112.81, 105.69, 105.07, 104.82, 103.37, 32.41, 28.54. IR (KBr, cm^{-1}): 3241, 1744, 1650, 1633, 1598, 1540, 1412, 1378, 1240, 1211, 1034, 988, 840, ESI-MS: *m/z* 437 [M^+ +1]. Anal. Calcd for $C_{22}H_{13}FN_2O_7$: C, 60.56; H, 3.00; F, 4.35; N, 6.42; O, 25.67. Found: C, 60.42; H, 3.23; F, 4.34; N, 6.41; O, 25.61. HRMS (ESI) calc. $C_{22}H_{13}FN_2NaO_7$ for [M^++Na] 459.0604, found: 459.0598.

4-(6,8-dichloro-4-oxo-4H-chromen-3-yl)-2-(methylamino)-3-nitropyrano[3,2-c]chromen-5(4H)-one(4f)

White solid; mp 280-282°C. 1H NMR (400 MHz, $CDCl_3$) δ 10.50 (d, *J* = 4.9 Hz, 1H), 8.47 (s, 1H), 7.98 – 7.83 (m, 2H), 7.71 – 7.59 (m, 2H), 7.46 – 7.35 (m, 2H), 5.07 (s, 1H), 3.46 (d, *J* = 5.3 Hz, 3H). ^{13}C NMR (100 MHz, $CDCl_3$) δ 175.60, 159.95, 158.91, 157.07, 153.89, 152.85, 150.55, 133.83, 133.20, 130.91, 126.08, 124.86,

124.71, 123.41, 122.33, 119.18, 117.23, 112.69, 105.33, 102.94, 32.38, 28.55. IR (KBr,cm^{-1}): 1336, 1860, 1755, 1680, 1568, 1370, 1265, 1080, 988, 815, 768. ESI-MS: *m/z* 487 [M$^+$+Na]. Anal. Calcd for $C_{22}H_{12}Cl_2N_2O_7$: C, 54.23; H, 2.48; Cl, 14.55; N, 5.75; O, 22.99. Found: C, 51.79; H, 2.37; Cl, 13.90; N, 5.49; Na, 4.51; O, 21.9. HRMS (ESI) calc. $C_{22}H_{13}Cl_2N_2O_7$ for [M$^+$+H] 487.0100, found: 487.0103.

4-(6-bromo-4-oxo-4H-chromen-3-yl)-2-(methylamino)-3-nitropyrano[3,2-c]chromen-5(4H)-one(4g)

White solid; mp 278-279°C. ^{1}H NMR (400 MHz, $CDCl_3$) δ 10.51 (d, *J* = 4.9 Hz, 1H), 8.40 (s, 1H), 8.15 (d, *J* = 2.4 Hz, 1H), 7.91 (dd, *J* = 7.9, 1.4 Hz, 1H), 7.70 (dd, *J* = 8.9, 2.4 Hz, 1H), 7.66 – 7.59 (m, 1H), 7.48 – 7.29 (m, 3H), 5.04 (s, 1H), 3.46 (d, *J* = 5.3 Hz, 3H). ^{13}C NMR (100 MHz, $CDCl_3$) δ 176.05, 159.99, 158.96, 157.18, 154.92, 153.79, 152.83, 136.64, 133.09, 127.93, 125.63, 124.80, 122.34, 120.31, 118.94, 118.67, 117.17, 112.75, 105.57, 103.18, 32.44, 28.54. IR (KBr,cm^{-1}): 3204, 1734, 1728, 1626, 1530, 1412, 1313, 1066, 1014, 950, 778, 648. ESI-MS: *m/z* 499 [M$^+$ +2]. Anal. Calcd for $C_{22}H_{13}BrN_2O_7$: C, 53.14; H, 2.64; Br, 16.07; N, 5.63; O, 22.52. Found: C, 52.92; H, 3.03; Br, 16.00; N, 5.61; O, 22.43. HRMS (ESI) calc. $C_{22}H_{13}BrN_2NaO_7$ for [M$^+$+Na] 518.9804, found: 518.9805.

4-(6-bromo-4-oxo-4H-chromen-3-yl)-9-methyl-2-(methylamino)-3-nitropyrano[3,2-c]chromen-5(4H)-one(4h)

White solid; mp 268-270°C. ^{1}H NMR (400 MHz, $CDCl_3$) δ 10.53 (s, 1H), 8.39 (s, 1H), 8.15 (d, *J* = 2.4 Hz, 1H), 7.75 – 7.61 (m, 2H), 7.42 (dd, *J* = 8.5, 1.7 Hz, 1H), 7.36 (d, *J* = 8.9 Hz, 1H), 7.24 (s, 1H), 5.04 (s, 1H), 3.47 (d, *J* = 5.2 Hz, 3H), 2.48 (s, 3H). ^{13}C NMR (100 MHz, $CDCl_3$) δ 176.03, 157.14, 154.93, 151.05, 136.61, 134.71, 134.12, 127.96, 121.92, 120.29, 119.00, 116.95, 112.43, 103.00, 32.43, 28.55, 21.10. IR (KBr, cm^{-1}): 3214, 2734, 2338, 1724, 1679, 1626, 1520, 1447, 1370, 1327, 1077, 835, 677, 658. ESI-MS: *m/z* 513 [M$^+$ +2]. Anal. Calcd for $C_{23}H_{15}BrN_2O_7$: C, 54.03; H, 2.96; Br, 15.63; N, 5.48; O, 21.91. Found: C, 53.82; H, 3.34; Br, 15.57; N, 5.46; O, 21.82. HRMS (ESI) calc. $C_{23}H_{15}BrN_2NaO_7$ for [M$^+$+Na] 532.9960, found: 532.9950.

9-methyl-4-(6-methyl-4-oxo-4H-chromen-3-yl)-2-(methylamino)-3-nitropyrano[3,2-c]chromen-5(4H)-one(4i)

White solid; mp 258-260°C. H NMR (400 MHz, $CDCl_3$) δ 10.56 (s, 1H), 8.37 (s, 1H), 7.66 (s, 1H), 7.42 (td, *J* = 8.7, 2.0 Hz, 3H), 7.35 (d, *J* = 8.5 Hz, 2H), 5.04 (s, 1H), 3.47 (d, *J* = 5.3 Hz, 3H), 2.47 (s, 3H), 2.36 (s, 3H). ^{13}C NMR (100 MHz, $CDCl_3$) δ 177.35, 160.20, 159.03, 156.91, 154.46, 153.64, 150.99, 135.13, 134.88, 134.61, 133.96, 124.44, 121.95, 118.48, 118.08, 116.83, 112.51, 105.87, 103.28, 32.45, 28.55, 21.08, 20.85, 18.42. IR (KBr, cm^{-1}): 3321, 1788, 1640, 1623, 1578, 1520, 1488, 1320, 1012, 988, 943, 890, 740. ESI-MS: *m/z* 447 [M$^+$ +1]. Anal. Calcd for $C_{24}H_{18}N_2O_7$: C, 64.57; H, 4.06; N, 6.28; O, 25.09. Found: C, 64.43; H, 4.28; N, 6.26; O, 25.03. HRMS (ESI) calc. for $C_{24}H_{18}N_2NaO_7$ [M$^+$+Na] 469.1012, found: 469.1015.

4-(6,8-dichloro-4-oxo-4H-chromen-3-yl)-9-methyl-2-(methylamino)-3-nitropyrano[3,2-c]chromen-5(4H)-one(4j)

White solid; mp 281-282°C. ^{1}H NMR (400 MHz, $CDCl_3$) δ 10.52 (d, *J* = 4.6 Hz, 1H), 8.46 (s, 1H), 7.88 (d, *J* = 2.5 Hz, 1H), 7.66 (dd, *J* = 6.2, 1.7 Hz, 2H), 7.43 (dd, *J* = 8.5, 1.7 Hz, 1H), 7.25 (s, 1H), 5.06 (s, 1H), 3.47 (d, *J* = 5.2 Hz, 3H), 2.48 (s, 3H). ^{13}C NMR (100 MHz, $CDCl_3$) δ 175.58, 160.13, 158.94, 157.03, 153.89, 151.06, 150.55, 134.78, 134.24, 133.79, 130.87, 126.10, 124.69, 123.42, 121.89, 119.25, 116.99, 112.36, 102.74, 32.37, 29.70, 28.58. IR (KBr, cm^{-1}): 1331, 1790, 1712, 1688, 1586, 1445, 1402, 1302, 1222, 1103, 974, 945, 850, 808, 740. ESI-MS: *m/z* 500 [M$^+$ +1]. Anal. Calcd for $C_{23}H_{14}C_{l2}N_2O_7$: C, 55.11; H, 2.82; Cl, 14.15; N, 5.59; O, 22.34. Found: C, 55.00; H, 3.01; Cl, 14.12; N, 5.58; O, 22.30. HRMS (ESI) calc.$C_{23}H_{14}Cl_2N_2NaO_7$ for [M$^+$+Na] 523.0076, found: 523.0078.

Acknowledgements

We thank TATA-CSIR-OSDD and CSIR, New Delhi, India for the financial support in the form of Senior Research Fellowship. The authors acknowledge the CSIR-CLRI for providing infrastructure to carry out this work.

Notes and references

1 P. Jithendra, A. M. Rajam, T. Kalaivani, A. B. Mandal and C. Rose, *ACS Appl. Mater. Interfaces.*, 2013, **5,** 7291.

2 R. Satieshkumar, P. Sathiamurthy, G. Arun, N. Anuya and S. Saravanan, B. Madhan, *ACS Appl.Mater.Interfaces.*, 2014, **6,** 15015.

3 J. Lin, C. Li, Y. Zhao, J. Hu and L. M. Zhang, *ACS Appl. Mater. Interfaces.*, 2012, **4,** 1050.

4 P. Agarwal, P. Srivastava, *Int. J. Biomed. Res.,* 2011, **2,** 181.

5 C. M. Murphy, M. G. Haugh, F. J. O. Brien, *Tissue Engineering, B. Med.,* 2010, **31,** 461.

6 B. Dillip Kumar, M. Santosh, V. Jayarama reddy and G. Soma, M. C. Kotturathu, R. Seeram, R. S. Verma, *J. Mater. Chem.,* 2013, **1,** 3972.

7 L. Ma, C. Gao, Z. Mao, J. Zhou, J. Shen and X. Hu, C. Han, *Biomaterials*., 2003, **24,** 4833.

8 J. A. Rameshw, Y. Y. Peng, V. Glattauer and J. A. Werkmesister, *J. Meter. Sci, Mater. Med.,* 2009, **20,** 3.

9 S. N. Park, J. C. Park, H. O. Kim and M. J. Song, H. Suh, *Biomaterials.,* 2002, **23,** 1205.

10 M. Peter, N. Ganeh, N. Selvamurugan, S. V. Nair and T. Furuike, H. Tamura, R. Jayakumar, *Carbohydrt. Polym.,* 2010, **80,** 687.

11 F. Chicatum, C. E. Pedraza, C. E. Ghezzi, B. Marelli and M. T. Kaartinen, M. D. Mckee, S. N. Nazhat, *Biomacromolecules.,* 2011, **12,** 2946.

12 W. Mattanavee, O. Suwantong, S. Puthong and T. Bunaprasert, V. P. Hoven, P. Supaphol, *ACS Appl.Mater. Interfaces.,* 2009, **1,** 1076.

13 Y. J. Hwang, J. Larsen, T. B. Krasieva and J. G. Lyubovitsky, *ACS Appl. Mater. Interfaces.,* 2011, **3,** 2579.

14 N. R. Rose, M. A. Mcdonough, O. N. F. King, A. Kawamura and C. J. Schofied, *Chem. Soc. Rev.,* 2011, **40,** 4364.

15 I. Kanungo, N. N. Fathima, R. R. Jonnalagadda and B. U. Nair, *Phys. Chem. Chem. Phys.,* 2015, **17,** 2778.

16 Y. B. Kim and G. H. Kim, *J. Mater. Chem. B.,* 2013, **1,** 3185.

17 G. Tronic, A. Doyel, J. Stephen, J. Russell and David, J. Wood, *Mater. Chem. B.,* 2013, **1,** 5478.

18 G. Tronic, A. Doyel, J. Stephen, J. Russell and David, J. Wood, *Mater. Chem. B.,* 2013, **1,** 3705.

19 S. Perumal, S. K. Ramadass, B. Madhan, *Eur. J. Pharm. Sci.,* 2014, **52,** 26.

20 H. J. Lee, S. H. Ahn and G. H. Kim, *ACS Chem. Mater.,* 2012, **24,** 881-891.

21 B. M. Novelo, J. L. M. Mata, A. V. Gonzalez, J. V. C. Rodriguez and A. M. Fernandez, *J. Mater. Chem. B*., 2014, **2,** 2874.

22 R. Sridhar, R. Lakshminarayanan, M. Kalaipriya, V. A. Bharathi, K. H. Chin Limh and R. S. Ramakrishan, *Chem. Soc. Rev.,* 2015, **44,** 790.

23 M. T. Alrifai, A. K. Shakya, K. A. Abu Safieh, M. S. Mubarak, *Med. Chem. Res.,* 2012, **21,** 468.

24 Y. Shi, C. H. Zhou, *Bioorg. Med. Chem. Leet.*. 2011, **21,** 956.

25 A. Rifai, A. A. Ayoub, M. T. Shakya, A. K. Abu Safieh, K. A. Mubarak, M. S., *Med. Chem. Res.,* 2012, **21,** 468.

26 (a) S. Thaisrivongs, M. N. Janakiraman, K. T. Chong, P. K. Tomich, L. A. Dolack, S. R. Turner and J. W. Strohbach, J. C. Lynn, M. M. Horng, R. R. Hinshaw, K. D. Watenpugh, *J.*

Med. Chem., 1996, **39,** 2400. (b) G. Rappa, K. Shyam, A. Lorico, O. Fodstad and A. C. Sartorelli, *Oncol. Res*., 2000, **12,** 113. (c) E. D Yang , Y. N. Zhao, K. Zhang and P. Mack, *Biochem. Biophys. Res. Commun.,* 1999, **260,** 682.

27 C. A. Kontogiorgis, D. J. Hadjipavlou Litina, *J. Med. Chem.,* 2005, **48,** 6400.

28 L. Pochet, C. Doucet, G. Dive, J. Wouters, B. Masereel, M. Reboud Ravaux, B. Pirotte, *Bioorg. Med.Chem.,* 2000, **8,** 1489.

29 E. Melliou, P. Magiatis, S. Mitaku, A. L. Skaltsounis, E. Chinou and I. Chinou, *J. Nat. prod.,* 2005, **68,** 78.

30 M. A. Azagarsamy, D. D. Makinnon and D. L. Alge, K. S. Anseth, , *ACS Macro Lett.,* 2014, **3,** 515.

31 A. Gaspar, M. J. Motos, j. Garrido, E. Uriarte and F. Borges, *Chem. Rev.,* 2014, **114,** 4960.

32 M. V. Kulkarni, G. M.Kulkarini, C. H. Lin, C. M. Sun, *Curr. Med. Chem.,* 2006, **13,** 2795.

33 B. V. Reddy, M. R. Reddy, C. H. Madan, K. P. Kumar, M. S. Rao. *Bioorg. Med .Chem. Lett.,* 2010, **20,** 7505.

34 J. J. J. Leahy, B. T. Golding, R. J. Griffin, I. R. Hardcastle, C. Richardson, L. Rigoreau and G. C. M. Smith, *Bioorg. Med. Chem. Litt.,* 2004, **14,** 6083.

35 M. Funke, D. Thimm, A. C. Schiedel and C. M. Muller, *J. Med. Chem.,* 2013, **56,** 5182.

36 M. V. S. N. Maddipatla, D. Wehrung, C. Tang, W. Fan, M. O. Oyewumi, T. Miyoshi and A. Joy, *ACS. Macromol.,* 2013, **46,** 5133.

37 S. R. Trenor, A. R. Shultz, B. J. Love and T. E. Long, *Chem. Rev.,* 2004, **104,** 3059.

38 S. Lee, S. Cho, M. Kim, G. Jin, U. Jeong and J. H. Jang, *ACS Appl. Mater. Interfaces.,* 2014, **6,** 1082.

39 A. Gaspar, M. J. Matos, J. Garrido, E. Uriarte and F. Borges, *ACS. Chem. Rev.,* 2014, **114,** 4960.

40 N. Yamamoto, N. S. Bryee, N. M. Nolte and T. W. Hambley, *ACS. Bioconjugate Chem.,* 2012, **23,** 1110.

41 C. M. Nimmo and M. S. Shoichet, *ACS Bioconjugate Chem.,* 2011**, 22,** 2199.

42 N. Duraipandy, R. Lakra, K. V. Srivatsan, U. Ramamoorthy, P. S. Korrapati, M. S. Kiran, *J. Mater. Chem B.,* 2015**, 3,** 1415.

43 Takeshi Nagai, Nobutaka Suzuki, *Food Chemistry*., 2000, **68,** 277.

44 Giriprasath Ramanathan, Sivakumar Singaravelu, M. D. Raja, S. S. Liji Sobhana and Uma Tirichurapalli Sivagnanam, *J. Biomater. Tiss. Eng*., 2014**, 4**, 203.

45 Sivakumar Singaravelu, Giriprasath Ramanathan, Raja. M. D, Sagar Barge and Uma Tirichurapalli, Materials letters, 2015, DOI: 10.10.16/j.matlat.2015.03.088.

46 Naveen Nagiah, Giriprasath Ramanathan and Tiruchirapalli SivagnanamUma. *Polym Tech.* 2013, **32,** 21370.

47 D. Archana.; Joydeep, Dutt.; P. K. Dutta. *Int J Biol Macromol.* 2013**, 57,** 193.

48 N. Nagiah, L. Madhavi, R. Anitha, N.T. Srinivasan, U.T. Sivagnanam, *Polym. Bull.* 2013, **70,** 2337.

49 J. Gong, F. Traganos, Z. Darzynkiewicz, *Anal Biochem.,* 1994, **218,** 314.

50 T. Mosmann, *J. Immunol. Methods.*, 1983, **65,** 55.

51 Limin Wang, Jan P. Stegemann, *Biomaterials*., 2010, **31,** 3976.

52 National Committee for Clinical Laboratory Standards, Methods for dilution antimicrobial susceptibility tests for bacteria that grow aerobically, 5th Edition, Approved Standard M7-A5. National Committee for Clinical Laboratory Standards, Wayne, Pa., 2000, **20,** 2.

53 M. R. Fazeli, G. Amin, M. M. A. Attar, H. Ashtiani, H. Jamalifar, N. Samadi, *Food Control.,* 2007, **18,** 646.

54 T. Muthukumar, R. Senthil, T.P. Sastry, Colloids Surf. B. Biointerfaces., 2013, **102,** 694.

55 Dongmei Luo, Lin Sang, Xiaoliang Wang, Songmei Xu, Xudong Li, Materials Letters 2011, **65**, 2395.

56 Nihal, Susana Breda, Erol Tasal, Cemil Ogratir, Rui Fausto, *Photochemistry and photobiology*., 2007, **83**, 1237.

57 N. Davidenko, J. J. Campbell, E.S. Thian, C.J. Watson, R.E. Cameron, *Acta Biomaterialia.,* 2010*,* **6**, 3957.

58 G. J. Khradi, *J. Anal. Calorim.,* 2012, **107**, 651.

59 Marilia M. Horn, Virginia C. Amaro Martins, Ana Maria de Guzzi Plepis, *Carbohydrt. Polym.,* 2009, **77**, 239.

60 F.Boccafoschi, J.Habermehl, S.Vesentini, D.Mantovani, Biomaterials, 2005, **26**, 7410.

61 Alina Sionkowska, Beata Kaczmarek, Katarzyna Lewandowska, *Journal of Molecular Liquids*, 2014, **199**, 318.

62 Ling Zhang, Kuifeng Li, Wenqian Xiao, Li Zheng, Yumei Xiao, Hongsong Fan, Xingdong Zhang, *Carbohydrt. Polym.,* 2011, **84**, 118.

63 A. Sionkowska, J. Kozłowska, *International Journal of Biological Macromolecules,* 2013, **52**, 250.

64 Giuseppe Falini, Simona Fermani, Elisabetta Foresti, Bruna Parma, Katia Rubini, Maria Chiara Sidotia, Norberto Rover, *J. Mater. Chem.,* 2004, **14**, 2297.

65 Florencia Chicatun, Claudio E. Pedraza, Naser Muja, Chiara E. Ghezzi, PhD, Marc D. McKee, Showan N. Nazha, *Tissue Engineering: Part A,* 2013, **19,** 2553.

66 Ruei-Yi Tsai, Ting-Yun Kuo, Shih-Chieh Hungb, Che-Min Lin, Tzu-Yang Hsiend, Da-Ming Wanga, Hsyue-Jen Hsieh, *Carbohydrt. Polym.,* 2015, **115**, 525.

67 Nandana Bhardwaj, Wan Ting Sow, Dipali Devi, Kee Woei Ng , Biman B. Mandal and Nam-Joon Cho, *Integrative Biology*, 2013, **7**, 142.

68 N. Nagiah, G. Ramanathan, L. Sobhana, U.T. Sivagnanam and N.T. Srinivasan *Int. J. Polym. Mater.,* 2014, **63**, 583.

69 Crystallographic data for the compound 4c in this manuscript have been deposited with the Cambridge Crystallographic Data Centre as supplementary publication number CCDC 1055442.

